Cancer Cell
Article

ATM Phosphorylation of Mdm2 Ser394 Regulates the Amplitude and Duration of the DNA Damage Response in Mice

Hugh S. Gannon,[1] Bruce A. Woda,[2] and Stephen N. Jones[1,3,*]
[1]Department of Cell Biology
[2]Department of Pathology
[3]Department of Cancer Biology
University of Massachusetts Medical School, Worcester, MA 01655, USA
*Correspondence: stephen.jones@umassmed.edu
DOI 10.1016/j.ccr.2012.04.011

SUMMARY

DNA damage induced by ionizing radiation activates the ATM kinase, which subsequently stabilizes and activates the p53 tumor suppressor protein. Although phosphorylation of p53 by ATM was found previously to modulate p53 levels and transcriptional activities in vivo, it does not appear to be a major regulator of p53 stability. We have utilized mice bearing altered *Mdm2* alleles to demonstrate that ATM phosphorylation of Mdm2 serine 394 is required for robust p53 stabilization and activation after DNA damage. In addition, we demonstrate that dephosphorylation of Mdm2 Ser394 regulates attenuation of the p53-mediated response to DNA damage. Therefore, the phosphorylation status of Mdm2 Ser394 governs p53 protein levels and functions in cells undergoing DNA damage.

INTRODUCTION

The p53 tumor suppressor has been called the "guardian of the genome" due to its ability to prevent genotoxic insults from inducing heritable alterations in damaged cells (Lane, 1992). In response to cellular stresses such as DNA double-strand breaks, hypoxia, and inappropriate oncogene activation, the p53 transcription factor is stabilized within the cell and induces the expression of various p53 target genes involved in cell cycle arrest, apoptosis, and senescence (Vousden and Lu, 2002). These p53-dependent effector pathways regulate the proliferation and propagation of damaged cells to limit cellular transformation and tumorigenesis, and mice deleted for p53 rapidly develop thymic lymphomas, sarcomas and other tumor types (Donehower et al., 1992). Additionally, over 50% of all human tumors harbor *p53* mutations (Soussi and Béroud, 2001; Hollstein et al., 1991). These findings clearly demonstrate the necessity of functional p53 signaling in suppressing tumorigenesis.

DNA damage induced by ionizing radiation (IR) is a well-established initiator of p53 activity. Wild-type (WT) mice that are treated with whole body IR undergo p53-dependent apoptosis in both radiosensitive tissues such as thymus, spleen, and small intestine, and in hematopoietic cells (Gudkov and Komarova, 2003). Mice exposed to 8 Grays (Gy) or more of IR will die within 3 weeks due to depletion of the hematopoietic compartment, a condition known as hematopoietic syndrome (Komarova et al., 2004). In contrast, *p53* null mice are more tolerant of acute radiation, as their hematopoietic cells are less prone to IR-induced apoptosis. However, *p53*-deficient mice will display an increased rate of tumorigenesis following IR treatment (Kemp et al., 1994).

Because p53-dependent cell cycle arrest and apoptosis are deleterious to the growth and survival of nondamaged cells, p53 activity must be kept at minimal levels under normal, homeostatic conditions. Although p53 regulation by numerous cellular proteins has been observed under various experimental conditions, it has become increasingly apparent that the Mdm2

Significance

The p53-mediated DNA damage response pathway suppresses the oncogenic transformation of cells exposed to genotoxic insults. A better understanding of the mechanisms that govern p53 activation during the DNA damage response is crucial to developing new cancer therapies, because tumors that harbor wild-type *p53* alleles have the potential for restoration of p53 activity, and because selectively regulating p53 functions might also ameliorate radiation therapy-induced pathologies. Our work determines that mouse Mdm2 Ser394 phosphorylation (human MDM2 Ser395) is required for DNA damage-induced p53 activation and also regulates the duration of the p53 response to DNA damage. Thus, devising means to alter the phosphorylation status of this residue should greatly facilitate our ability to regulate p53 activity in normal and neoplastic cells.

oncoprotein is the chief negative regulator of p53 in damaged and nondamaged cells (Bond et al., 2005). Mdm2 represses p53 activity by binding and sequestering p53 away from p53 target gene promoters (Momand et al., 1992; Chen et al., 1995). Furthermore, Mdm2 contains a RING domain with E3 ubiquitin ligase activity and can ubiquitinate p53, leading to p53 nuclear export and degradation in the 26S proteasome (Honda et al., 1997). Interestingly, Mdm2 is a transcriptional target of p53, and p53 transactivation of *Mdm2* expression is thought to form an autoregulatory feedback loop to limit p53 activity in the cell (Juven et al., 1993; Wu et al., 1993). The importance of Mdm2-mediated inhibition of p53 signaling has been demonstrated previously in vivo. $Mdm2^{-/-}$ mice die at E5–E6 during development due to aberrant p53-mediated apoptosis (Jones et al., 1995; Montes de Oca Luna et al., 1995), whereas Mdm2 overexpression in mice inhibits p53 tumor suppression, resulting in the formation of lymphomas, soft tissue sarcomas, and osteosarcomas (Jones et al., 1998). Thus proper regulation of Mdm2 expression and activity is critical for normal p53 signaling and cellular function.

Activation of p53 in response to DNA damage necessitates a transient attenuation of Mdm2-dependent p53 inhibition. Posttranslational modifications of the p53 protein by DNA damage-inducible kinases were initially thought to inhibit the interaction of p53 and Mdm2 (Shieh et al., 1997). The ATM (mutated in ataxia and telangiectasia) kinase is necessary for p53 stabilization in tissues such as mouse embryonic fibroblasts (MEFs) and murine thymus following IR (Jack et al., 2002; Gurley and Kemp, 2007), and ATM will directly and indirectly (via Chk2) phosphorylate p53 on Ser18 and Ser23 in irradiated mice (Ser15 and Ser20 on human p53) (Chao et al., 2000; Wu et al., 2002). These serine residues are located within or adjacent to the Mdm2 binding domain of p53, and initial in vitro studies demonstrated that phosphorylation of p53 decreased the p53-Mdm2 interaction in transfection and overexpression experiments (Shieh et al., 1997). Several groups, including our own, subsequently generated mouse models bearing modified *p53* alleles to examine the role of these posttranslational modifications in p53 regulation and function in vivo (Chao et al., 2003, 2006; Sluss et al., 2004). These studies revealed that phosphorylation of these ATM-target serines on p53 modulated the transcriptional activity of p53, but had only a moderate effect on DNA damage-induced stabilization of the p53 protein.

In addition to modifying p53, transfection-based assays have revealed that ATM can directly phosphorylate serine 395 of human MDM2 (Khosravi et al., 1999; Maya et al., 2001). One study utilized an *MDM2* expression construct with the serine residue 395 codon replaced by sequences encoding aspartic acid (S395D), thus mimicking a constitutively phosphorylated serine residue. The MDM2 S395D protein exhibited a decreased capacity to induce p53 degradation and nuclear export, suggesting that phosphorylation of MDM2 Ser395 altered p53 activation following DNA damage. Further in vitro work suggested that ATM phosphorylation of multiple amino acid residues on MDM2, including Ser395, inhibited both MDM2 RING domain oligomerization and E3 ligase activity (Cheng et al., 2009, 2011). Interestingly, recent work has indicated that ATM phosphorylation of MDM2 switches MDM2 from a negative to a positive regulator of p53, as phosphorylation of MDM2 Ser395 increased the interaction between MDM2 protein and *p53* mRNA and led to increased p53 translation (Gajjar et al., 2012). These transfection-based studies suggest that the ATM-dependent induction of the p53 protein is mediated by ATM phosphorylation of MDM2.

In keeping with a role for MDM2 Ser395 phosphorylation in the p53 DNA damage response, we have previously shown that the Wip1 oncoprotein can dephosphorylate MDM2 Ser395 in vitro (Lu et al., 2007). Wip1 antagonizes ATM function by dephosphorylating many known ATM target proteins, including ATM itself. Therefore, Wip1 has been proposed to reset DNA damage signaling to prestress levels following resolution of the DNA damage response (Lu et al., 2008). Like Mdm2, the Wip1 gene is a direct transcriptional target of p53, and p53 induction of *Wip1* expression might also limit the p53-dependent DNA damage response. Although the coincidental timing of MDM2 Ser395 phosphorylation and dephosphorylation suggests that this modification may coordinate the p53-dependent response to DNA damage, the in vivo functional significance MDM2 phosphorylation in Mdm2-p53 regulation, p53 activation, and in tumorigenesis remains unknown.

To determine the role of MDM2 Ser395 phosphorylation in p53 regulation under physiological settings, we have generated two knock-in mouse models bearing *Mdm2* Ser394 substitutions (the orthologous human Ser395 residue in the mouse) and analyzed the effects of these substitutions on p53-mediated DNA damage response and tumor suppression.

RESULTS

To investigate the role of Mdm2 Ser394 phosphorylation under physiological conditions, we generated a mouse model in which this serine residue is substituted with an alanine residue (*S394A*). This model produces a mutant Mdm2 protein with a conserved native structure that cannot be phosphorylated at position 394. Site-directed mutagenesis was performed to introduce missense mutations within the 394 codon of *Mdm2* exon 12, and a gene-replacement vector was constructed to replace the endogenous *Mdm2* exon 12 sequences with a mutated exon 12 (Figure 1A). The introduced mutations also inserted a novel *BcgI* restriction digest site at codon 394, which allows direct detection of the mutated sequence by a PCR strategy. Gene targeting experiments in PC3 (129SV) embryonic stem (ES) cells (O'Gorman et al., 1997) yielded properly-targeted ES cell clones, as confirmed by Southern and PCR analyses (Figures S1A–S1C available online). Blastocyst injection experiments produced several high-degree male chimeras that passed the *S394A* allele through their germ line while simultaneously deleting the floxed neomycin cassette due to expression of the protamine-Cre transgene (present in the PC3 ES cells). The resultant F_1 and F_2 generation mice were identified by Southern blot of genomic DNA (Figure S1D). The presence of the *S394A* mutation in these mice was confirmed by utilizing the PCR-*BcgI* digest strategy (Figure 1B). This corroborated the Southern genotyping results and demonstrated retention of the mutation in both heterozygous (*A*/+) and homozygous (*A*/*A*) mice. All genotyping techniques were reaffirmed by direct genomic sequencing of the exon 12 region in F_1 and F_2 mouse genomic DNA (Figure S1E).

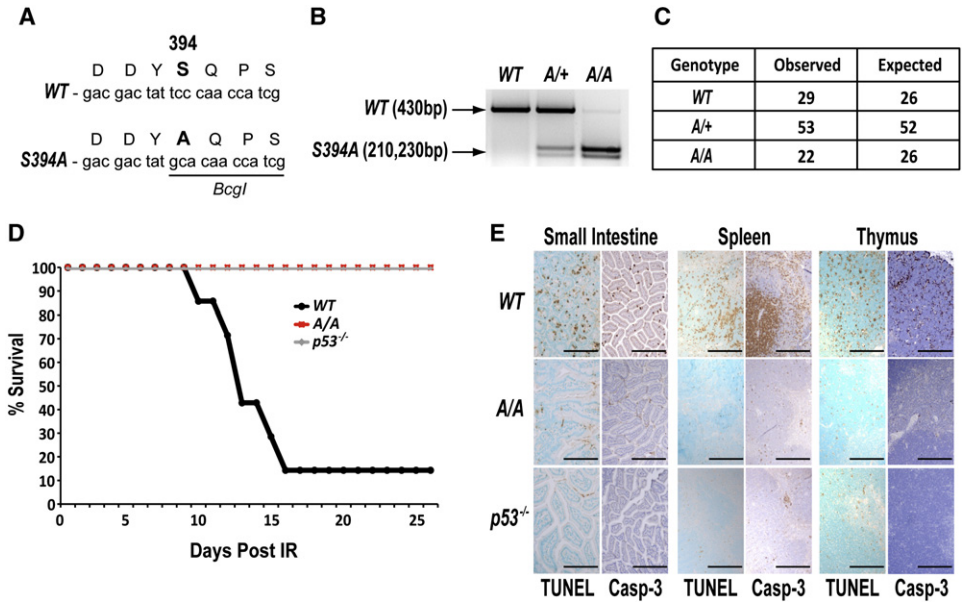

Figure 1. Phosphorylation of Mdm2 Ser394 Regulates Radiosensitivity in Mice

(A) DNA sequence of the *WT* and *S394A* alleles at *Mdm2* codon 394. The mutations in *S394A* also introduce a *BcgI* restriction digest site.

(B) PCR-*BcgI* analysis of F_2 generation mice. Primers flanking *Mdm2* codon 394 were used to amplify DNA samples from *WT*, *A*/+, and *A/A* F_2 generation mice, followed by *BcgI* digestion.

(C) Mice that are either heterozygous and homozygous for the *S394A* allele are viable and were observed at Mendelian ratios after heterozygous intercrosses ($p = 0.322$).

(D) Cohorts of wild-type (n = 14), *A/A* (n = 14), and $p53^{-/-}$ (n = 8) mice were irradiated with 8Gy and survival was observed over 26 days.

(E) *WT*, *A/A*, and $p53^{-/-}$ mice were irradiated with 2Gy and were sacrificed 6 hr later. Small intestine, spleen, and thymus were harvested and stained for TUNEL or anti-cleaved caspase-3 (Casp-3). Scale bars represent 250 μm.

See also Figure S1.

A/+ and *A/A* mice are viable and were recovered from heterozygous intercrosses at Mendelian ratios (Figure 1C). Because $Mdm2^{-/-}$ mice are embryonic lethal (Jones et al., 1995; Montes de Oca Luna et al., 1995), total ablation of Mdm2 function during development must not be occurring in *A*/+ or *A/A* mice. We also did not detect any differences between *WT* and *A/A* mice in body weights at 8 weeks of age (*WT* 25.67 ± 2.9 g and *A/A* 24.3 ± 4.2 g), in male-to-female sex distribution (*WT* 1:0.82 and *A/A* 1:0.90), or in overall litter size (*WT* 8.5 ± 1.8 and *A/A* 8.7 ± 1.9). Because mice with decreased p53 function have decreased fecundity (Levine et al., 2011), our results suggest that basal p53 activity is not perturbed in *A/A* mice.

Because ATM phosphorylation of MDM2 Ser395 was previously observed in cell lines following IR treatment (Maya et al., 2001), we assessed the sensitivity of *A/A* mice to whole body γ-irradiation. We irradiated cohorts of *WT*, *A/A*, and $p53^{-/-}$ mice with a threshold-lethal dose of IR (8Gy). As expected, 86% of wild-type mice died by 16 days post-IR (Figure 1D). However, like $p53^{-/-}$ mice, *A/A* mice were completely radioresistant, indicating that Mdm2 Ser394 phosphorylation regulates p53 activity in vivo following DNA damage. Activation of p53 by IR damage in mice induces apoptosis in radiosensitive organs such as small intestine, spleen, and thymus (Gudkov and Komarova, 2003). To evaluate p53 apoptotic function in these tissues, we treated *WT*, *A/A*, and $p53^{-/-}$ mice with 2Gy IR and 6 hr later assayed apoptosis by terminal deoxynucleotidyl transferase dUTP nick end labeling (TUNEL) and cleaved caspase-3 immunohistochemistry (Figure 1E). Very few apoptotic cells were detected in the small intestine, spleen, or the thymus of *A/A* mice following DNA damage, whereas apoptosis was readily apparent in all of these tissues in irradiated wild-type mice. As expected, little or no apoptosis was observed in tissues of IR-treated $p53^{-/-}$ control mice, and apoptosis was not detected in the untreated animals, regardless of genotype (Figure S1F). These studies indicate markedly reduced p53-dependent apoptotic function in *A/A* mice after IR treatment.

To more accurately quantitate this IR-dependent effect, we utilized Annexin V and propidium iodide (PI) staining to assay apoptosis in ex vivo thymocytes by flow cytometry (Figure S2A). Wild-type thymocytes are sensitive to apoptosis due to p53-induced activation of proapoptotic *Puma* expression (Jeffers et al., 2003). In agreement with the whole-body IR results, *WT* thymocytes treated with 2Gy IR displayed 3.1-fold more early apoptotic (Annexin V^{high} PI^{low}) cells at 12 hr compared to untreated *WT* cells, whereas *A/A* thymocytes displayed only a modest 1.5-fold increase in apoptotic cells and $p53^{-/-}$ thymocytes showed no induction of apoptosis after DNA damage (Figure 2A).

To establish that the decreased apoptosis in DNA damaged *A/A* thymocytes is due to altered p53 function, we treated *WT*, *A/A*, and $p53^{-/-}$ thymocytes with Nutlin-3a, a small-molecule inhibitor of Mdm2-p53 binding (Vassilev et al., 2004). *WT* and *A/A* thymocytes cotreated with Nutlin-3a and IR each stabilized p53 after IR damage (Figure 2B), and blocking the interaction of

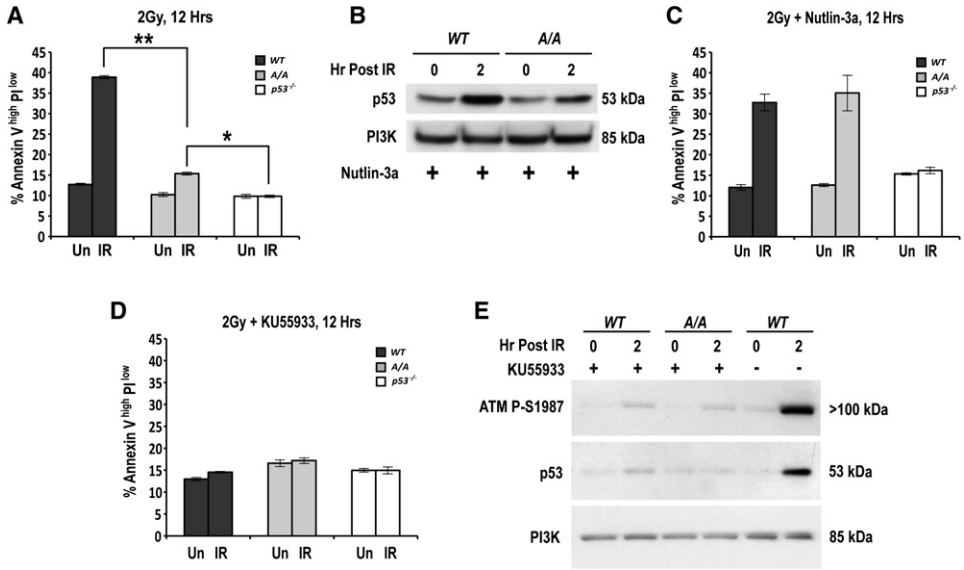

Figure 2. ATM Phosphorylation of Mdm2 Ser394 Promotes p53-Dependent Apoptosis after DNA Damage

(A) Ex vivo thymocytes were either left untreated or irradiated with 2Gy for 12 hr and apoptotic cells were quantified by flow cytometry (n = 3 per genotype). Standard deviation indicated by error bars. Asterisk (p = 0.0001) and double asterisk (p = 0.0001) indicate significant differences.

(B) Ex vivo thymocytes were either untreated or irradiated with 2Gy for 1 hr, and all cells were then incubated with 12 μM Nutlin-3a for 1 hr. Protein levels were analyzed by western blot.

(C) Ex vivo thymocytes were either left completely untreated or irradiated with 2Gy for 12 hr and incubated with 12 μM Nutlin-3a 3 hr after IR (9 hr total) (n = 3 per genotype). Apoptotic cells were quantified by flow cytometry Standard deviation indicated by error bars.

(D) Ex vivo thymocytes were preincubated with 10 μM KU55933 for 1 hr. Cells were then either left untreated or irradiated with 2Gy for 12 hr and apoptotic cells were quantified by flow cytometry (n = 3 per genotype). Standard deviation indicated by error bars.

(E) Ex vivo thymocytes were either left untreated or preincubated with 10 μM KU55933 for 1 hr. Cells were then either untreated or irradiated with 2Gy for 2 hr, and protein levels were analyzed by western blot.

See also Figure S2.

p53 with Mdm2-S394A completely rescued the ability of p53 to induce apoptosis in *A/A* thymocytes following DNA damage (Figure 2C). To confirm that Nutlin-3a treatment restored IR-induced apoptosis in *A/A* cells by inhibiting Mdm2-p53 signaling, we performed FACS analysis on *A/A* thymocytes that were genetically deleted for p53. As expected, the addition of Nutlin-3a failed to restore IR-induced apoptosis in *A/A* cells lacking *p53* (Figure S2B).

To verify that the effect of the *Mdm2 S394A* mutation on IR-apoptosis was truly ATM-dependent, we repeated the apoptosis assays using the ATM-specific inhibitor KU55933 (Hickson et al., 2004). Inhibition of ATM reduced apoptosis in irradiated thymocytes to levels observed in untreated cells in all genotypes (Figure 2D). Additionally, the ATM inhibitor blocked the robust ATM activation and p53 protein stabilization induced by IR damage (Figure 2E).

To further investigate the lack of IR-induced p53 function in *A/A* mice, we compared the stabilization and activity of p53 in *WT* and *A/A* radiosensitive tissues after DNA damage. We first harvested whole spleen protein extracts 4 hr after whole-body IR treatment. As expected, activation of the ATM kinase in wild-type mice by 4Gy IR was readily detected, as judged by the extent of autophosphorylated ATM Ser1987, the mouse ortholog of human ATM Ser1981 (Pellegrini et al., 2006), and this tissue displayed robust IR-stabilization of p53 (Figure 3A). However, *A/A* mice lack any detectable stabilization of the p53 protein, despite comparable activation of ATM by IR. This lack of p53 protein upregulation in IR-treated *A/A* spleen extracts was seen in multiple mice (Figure S3A), and corresponded with greatly decreased induction of the p53-target genes *Puma*, *p21*, *Bax*, and *Noxa*, as measured by quantitative real time PCR (qRT-PCR) (Figure 3B). However, IR-treated *A/A* spleens did show a low-level activation of p53, as expression of p53 target genes was slightly elevated relative to levels in IR-treated $p53^{-/-}$ spleens.

Similar results were seen at multiple time points in thymus extracts following whole-body IR treatment of mice (Figures 3C and S3B). The level of p53 protein in wild-type thymus was upregulated by 6.4-fold (1 hr), 4.8-fold (2 hr), and 1.8-fold (4 hr) following 4Gy IR, whereas p53 levels in IR-treated *A/A* thymus were upregulated by only 2.1-fold, 1.3-fold, and 1.2-fold at these respective time points (Figure 3C). Again, these differences were seen despite similar activation of the ATM kinase. As observed in spleen, expression of the p53-target genes *Puma* and *p21* were significantly reduced in *A/A* thymus at all time points after IR treatment (Figure 3D). Because the p53 protein is phosphorylated by ATM on p53 Ser18 in the treated *A/A* thymus (Figure 3C), the reduced levels of p53 target gene expression in this tissue are likely due to decreased p53 protein stabilization in *A/A* mice after IR, and not due to failure of ATM to induce proper posttranslational modification of p53. Analysis of multiple p53 target genes in irradiated *WT* and *A/A* thymocytes using p53

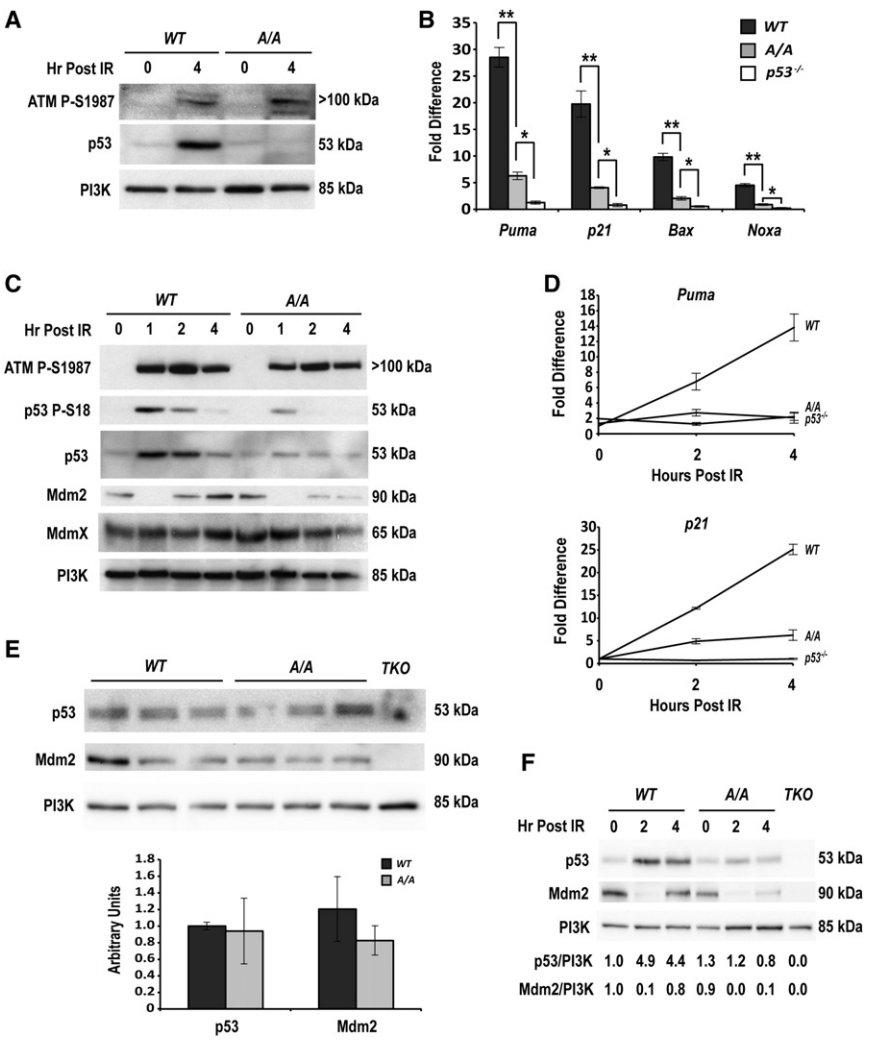

Figure 3. Mdm2 Ser394 Phosphorylation Is Necessary for p53 Stability and Activity after DNA Damage

(A) Mice were either untreated or irradiated with 4Gy and spleens were harvested 4 hr later. Protein levels were then analyzed by western blot.

(B) Mice were either untreated or irradiated with 4Gy and spleens were harvested 4 hr later (n = 3 per genotype). Relative expression levels of p53 target genes in irradiated spleen extracts were determined by qRT-PCR. Levels were normalized to untreated wild-type and are presented as the ratio of mRNA to *Gapdh* mRNA. Standard deviation indicated by error bars. Asterisks indicate a significant difference: double asterisk *Puma* p = 0.002, *p21* p = 0.01, *Bax* p = 0.003, *Noxa* p = 0.002; single asterisk *Puma* p = 0.01, *p21* p = 0.001, *Bax* p = 0.01, *Noxa* p = 0.008.

(C) Mice were either untreated or irradiated with 4Gy and thymi were harvested at the indicated times. Protein levels were then analyzed by western blot.

(D) Mice were either untreated or irradiated with 4Gy and thymi were harvested 2 or 4 hr later (n = 3 per genotype). Relative expression levels of p53 target genes were determined by qRT-PCR. Data are presented as the ratio of mRNA to *Gapdh* mRNA. Standard deviation indicated by error bars. Significant differences were seen between *WT* and *A/A Puma* at 2 (p = 0.035) and 4 (p = 0.002) hr and between *WT* and *A/A p21* at 2 (p = 0.0001) and 4 (p = 0.0001) hr.

(E) Protein levels from whole thymus extracts from untreated mice were analyzed by western blot (n = 3 per genotype). Quantified levels of p53 (p = 0.83) and Mdm2 (p = 0.11) relative to PI3K were normalized to wild-type.

(F) Mice were either untreated or irradiated with 4Gy and thymi were harvested at the indicated times. Protein levels were then analyzed by western blot. Quantified levels of p53 and Mdm2 relative to PI3K were normalized to untreated wild-type.

See also Figure S3.

signaling pathway PCR arrays confirmed reduced activation of multiple p53 target genes in treated *A/A* cells (Figure S3C). These results reveal that Mdm2 Ser394 phosphorylation is required in vivo for p53 stabilization and robust p53 activation after DNA damage.

Mdm2 destabilization in response to DNA damage has been shown previously (Stommel and Wahl, 2004), and we observed an initial decrease in Mdm2 protein in both *WT* and *A/A* tissues. Interestingly, these Mdm2 levels recovered at 2 and 4 hr in both genotypes, with more Mdm2 protein being present in *WT* at these times compared to *A/A* (Figure 3C). To determine if the initial decrease in Mdm2 levels was due to epitope masking by IR-induced phosphorylation, we treated these extracts with calf intestinal phosphatase (CIP); however, this treatment neither increased nor altered the pattern of Mdm2 levels after DNA damage (Figure S3D). Interestingly, the phosphorylation status of Mdm2 Ser394 had no effect on the levels of MdmX, an Mdm2-related p53 regulatory protein, in this tissue. The specificities of the Mdm2 and MdmX antibodies were validated using *Mdm2*$^{-/-}$, *MdmX*$^{-/-}$, *p53*$^{-/-}$ triple-knockout (*TKO*) thymus extracts (Figure S3E).

We next wanted to determine why differences in p53 and Mdm2 levels are observed in irradiated *WT* versus *A/A* cells. One possibility is that p53 and Mdm2 protein levels are initially lower in *A/A* cells than in *WT* cells, leading to an overall reduced DNA damage response in *A/A* mice. To test this, we carefully quantitated p53 and Mdm2 protein levels in untreated *WT* and *A/A* whole thymus extracts and found no significant difference in the levels of either p53 or Mdm2 proteins at baseline (Figure 3E). These data support the similar baseline levels of apoptosis and gene expression that we observed in *WT* and *A/A* tissues in the absence of DNA damage (Figures 2 and 3E). Furthermore, careful quantitation confirmed that there is less p53 protein and Mdm2 protein in *A/A* thymus than in *WT* thymus after IR (Figure 3F). Because baseline Mdm2 levels were equivalent in *A/A* and *WT* tissue, the reduced amount of Mdm2 and p53 in *A/A* versus *WT* tissues reflects a specific difference in the response of *A/A* cells to DNA damage.

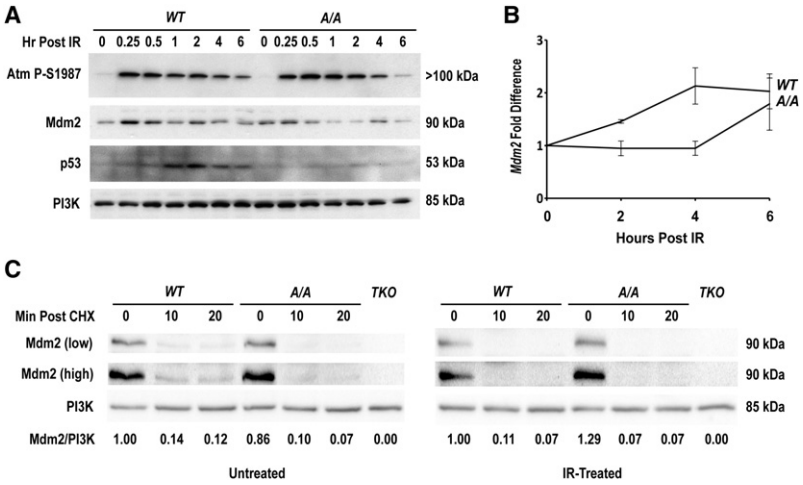

Figure 4. Phosphorylation of Mdm2 Ser394 Does Not Significantly Impact Mdm2 Destabilization after DNA Damage

(A) Ex vivo thymocytes were either untreated or irradiated with 2Gy for the indicated times. Protein levels were then analyzed by western blot.

(B) Ex vivo thymocytes were either untreated or irradiated with 2Gy for the indicated time points (n = 3 per genotype). Relative expression levels of *Mdm2* were determined by qRT-PCR. Data are presented as the ratio of mRNA to *Gapdh* mRNA. Standard deviation indicated by error bars.

(C) Ex vivo thymocytes were incubated with 50 μg/ml of CHX and either left untreated or irradiated with 2Gy for the indicated times. Protein levels were then analyzed by western blot. Quantified levels of Mdm2 relative to PI3K were normalized to untreated wild-type.

See also Figure S4.

To further examine the effects of Mdm2 Ser394 phosphorylation on p53 and Mdm2 stability, we performed western blots using irradiated *WT* and *A/A* ex vivo thymocytes. Stabilization of p53 was detected in primary wild-type thymocytes at 1–2 hr post-IR, and p53 levels remained elevated in these cells 6 hr after IR damage (Figures 4A and S4). In contrast, p53 stabilization was not apparent in *A/A* thymocytes at these early time points after DNA damage, even though ATM was clearly activated by IR treatment. Similar to whole thymus extracts, Mdm2 levels also appear decreased in irradiated *A/A* thymocytes compared to IR-treated *WT* cells. The increased levels in wild-type Mdm2 protein may be due to increased p53-induced *Mdm2* transcription, and indeed, like other p53-dependent targets, *Mdm2* transcripts are lower in the irradiated *A/A* thymocytes (Figure 4B). Alternatively, the difference in Mdm2 protein levels after DNA damage may be due to decreased Mdm2 protein stability in *A/A* thymocytes compared to *WT* cells. To examine the effects of Mdm2 Ser394 phosphorylation on Mdm2 stability in vivo, we incubated untreated and irradiated *WT* and *A/A* thymocytes with the protein synthesis inhibitor cycloheximide (CHX). Although Mdm2 protein is relatively unstable in thymocytes, we found that IR treatment lead to further decreases in Mdm2 stability in both genotypes (Figure 4C). However, the stability of Mdm2 proteins in untreated and IR-treated *WT* and *A/A* thymocytes was comparatively indistinguishable. Therefore, our results indicate that the lower Mdm2 protein levels in *A/A* thymocytes after DNA damage reflects less p53 activation of *Mdm2* transcription in these cells and not reduced Mdm2-S394A protein stability.

The reduced p53 transactivation of *p21* observed in the spleen and thymus of IR-treated *A/A* mice (Figure 3) suggests that Mdm2 Ser394 phosphorylation may also impact p53 regulation of cell proliferation. To examine this further, we assayed p53 function in *WT* and *A/A* MEFs. No difference in the growth rate of *A/A* or *WT* cells was observed using a standard proliferation assay (Figure 5A). This result is in keeping with the equivalent low levels of p53 observed in nondamaged *WT* and *A/A* tissues (Figure 3). However, greater p53 protein stabilization was observed in *WT* MEFs than in *A/A* MEFs at 6 and 12 hr post-IR (Figure 5B). Likewise, transactivation of *p21* was greater in *WT* MEFs than in *A/A* cells, and induction of *Mdm2* transcripts was delayed in *A/A* MEFs (Figure 5C). FACS analysis of *WT*, *A/A*, and $p53^{-/-}$ MEFs at 18 and 45 hr post-IR revealed that *A/A* cells are compromised in their ability undergo growth arrest after DNA damage (Figure 5D). However, as compared to $p53^{-/-}$ cells, the *A/A* MEFs do retain the ability to undergo a partial growth arrest after IR damage. Additionally, no differences were observed in the nuclear versus cytoplasmic fraction of Mdm2 protein in *A/A* and *WT* MEFs before or after DNA damage (Figure S5). These data reveal that phosphorylation of Mdm2 Ser394 also governs the ability of Mdm2 to regulate p53-mediated cell growth arrest after IR.

Because ATM phosphorylation of Mdm2 Ser394 is necessary for robust p53 activation after DNA damage, we wanted to test whether this posttranslational modification alone was sufficient to induce p53 activity in untreated tissues. To this end, we generated a different mouse model in which *Mdm2 Ser394* was mutated to aspartic acid (*S394D*), thus mimicking a constitutively phosphorylated serine residue (Figure 6A). We followed the same gene replacement strategy used to generate the *S394A* model (Figures S6A–S6D). We hypothesized that if phosphorylation of Mdm2 Ser394 is sufficient by itself to disrupt Mdm2 regulation of p53, then substitution of aspartic acid at codon 394 might lead to embryonic lethality in mice bearing functional *p53* alleles (as is seen in *Mdm2* null mice). However, both heterozygous (*D/+*) and homozygous (*D/D*) mice proved to be viable, and both genotypes were recovered from heterozygous intercrosses at Mendelian ratios (Figure S6E). The viability of this knock-in mutant suggests that baseline levels of p53 protein would be unchanged in this model compared to controls, and subsequent quantitation of p53 and Mdm2 protein levels in untreated thymus protein extracts revealed no significant differences between *WT* and *D/D* (Figure 6B).

The viability of *D/D* mice also suggests that either multiple DNA damage signals are needed to attenuate Mdm2 regulation and activate p53, or that the *Mdm2 S394D* mutation poorly mimics a phosphoserine residue. The latter possibility would result in *D/D* mice presenting with phenotypes similar to our *A/A* model, because aspartic acid (like alanine) cannot be phosphorylated. To test this, we treated *WT* and *D/D* mice with 4Gy whole-body irradiation and examined p53 stabilization in thymus cells at various early time points after DNA damage. In contrast

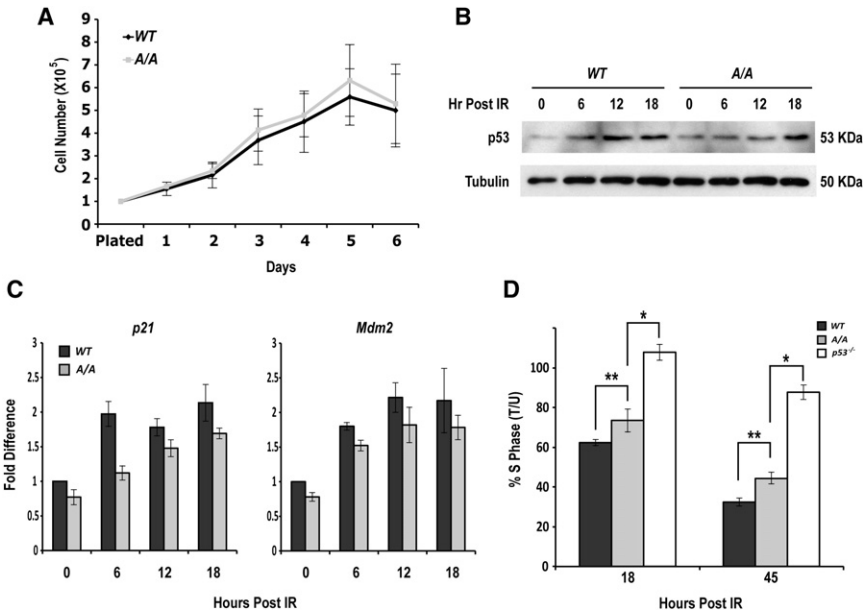

Figure 5. Mdm2 Ser394 Phosphorylation Is Necessary for Full p53 Stabilization and Function in MEFs

(A) Primary MEFs proliferation was counted each day (n = 3 per genotype). Standard deviation indicated by error bars.

(B) Primary MEFs were either untreated or irradiated with 4Gy for the indicated times, and protein levels were then analyzed by western blot.

(C) Primary MEFs were either untreated or irradiated with 4Gy for the indicated times (n = 3 per genotype). Relative expression levels of p53 target genes were determined by qRT-PCR. Data are presented as the ratio of mRNA to *Gapdh* mRNA. Standard deviation indicated by error bars.

(D) Primary MEFs were treated with 4Gy IR for the indicated time points and then incubated with bromodeoxyuridine (BrdU) for 3 hr (n = 3 per genotype). Cells were then analyzed by flow cytometry. Standard deviation indicated by error bars. Asterisks indicate a significant difference: double asterisk 18 hr p = 0.0318, 45 hr p = 0.0126; single asterisk 18 hr, p = 0.0004, 45 hr p = 0.0001. See also Figure S5.

to what we observed in *A/A* cells, p53 protein stabilization by IR damage in *D/D* thymus extracts was comparable to wild-type (Figure 6C). This was also observed in IR-treated ex vivo thymocytes (Figure S6F). Likewise, the pattern of Mdm2 protein destabilization followed by recovery was equivalent between the *WT* and *D/D* tissues (Figure 6C), which reflects the equal induction of *Mdm2* transcript levels seen in DNA damaged thymocytes (Figure 6D). *Puma* transcript levels were also similarly increased in the IR-treated *WT* and *D/D* cells (Figure 6D), and the levels of DNA damage-induced apoptosis were the same between *WT* and *D/D* thymocytes at 12 hr after IR treatment (Figure 6E). Similar results were obtained in thymocytes at 24 hr post-IR (Figure S5G), as well as in thymocytes isolated 48 hr after whole-body IR in *WT*, *D/D*, and $p53^{-/-}$ mice (Figure S5H). Collectively, these findings demonstrate that *Mdm2 S394D* mimics the effects of the phosphorylated Mdm2 Ser394 protein in wild-type mice after DNA damage. As baseline levels of p53 protein and apoptosis in nondamaged *WT* and *D/D* cells are the same in these assays, the mimicking of Mdm2 Ser394 phosphorylation in *D/D* thymocytes is not sufficient in the absence of other DNA damage-induced signals to induce p53 activation.

To confirm the effects of this Mdm2 Ser394 phospho-mimic in cell growth, *WT* and *D/D* MEFs were analyzed for cell proliferation (Figure 6F). As with *A/A* MEFs, the *D/D* MEFs proliferated at the same rate as wild-type MEFs in culture. However, IR-treatment of *D/D* MEFs induced p53 stabilization at levels similar to IR-treated *WT* MEFs (Figure 6G), and IR damage induced an equivalent p53-mediated reduction in S phase in both *WT* and *D/D* cells (Figure 6H).

Previous in vitro work has established that the Wip1 phosphatase can dephosphorylate multiple ATM targets, including human ATM Ser1981, p53 Ser15, and MDM2 Ser395 (Shreeram et al., 2006; Lu et al., 2005, 2007). This dephosphorylation has been proposed to return DNA damage signaling to basal levels once the DNA damage has been resolved. Because Wip1 cannot dephosphorylate the Mdm2-S394D residue, we hypothesized that *D/D* and *WT* mice might have differences in the duration of Mdm2-p53 signaling after IR treatment. Therefore, we analyzed p53 stabilization and activity at later time points in the DNA damage response. Like *D/D* thymocytes (Figure S6F), *WT* and *D/D* spleen samples had equal levels of ATM activity and p53 levels at 4 hr post-IR. However, the level of p53 protein remained persistently elevated at 8 hr post-IR in *D/D* extracts, despite the reduction in ATM activity and similar levels of Mdm2 by this later time point (Figures 7A and S7A). A similar response pattern was seen in primary thymocytes. Although p53 was stabilized to a similar extent in *WT* and *D/D* mice at early time points after IR damage (see Figure 6C), p53 levels remain elevated in *D/D* thymocytes at 12 hr post-IR, whereas p53 stabilization is less obvious at this later time point in wild-type cells (Figure 7B). As in spleen, the elongated duration of p53 stabilization in *D/D* thymocytes was seen well after resolution of the DNA damage response, as indicated by the absence of phospho-ATM at 12 hr post-IR, and despite the presence of Mdm2. The elongated p53 response in *D/D* thymocytes was reflected by increased levels of *Puma*, *p21*, *Mdm2*, and *Wip1* expression found in these cells at 12 and 18 hr post-IR (Figure 7C), and p53 signaling pathway PCR array analysis of additional p53 target genes confirmed that p53 activation remained elevated in *D/D* thymocytes relative to wild-type levels at 12 hr following IR (Figure S7B).

Finally, to explore the importance of Mdm2 Ser394 phosphorylation in p53-mediated tumor suppression, we established cohorts of *WT*, *A/A*, and *D/D* mice and performed a tumor assay. In 24 months, 20 of 31 (65%) *A/A* mice developed spontaneous tumors, whereas only 1 of 24 (4%) *D/D* mice presented with a tumor of the salivary gland epithelium (Figure 8A). None of the wild-type mice presented with a tumor during this interval. Most of the *A/A* tumors arose between 18–24 months of age, which closely resembles previous $p53^{+/-}$ tumor curves (Harvey et al., 1993; Jacks et al., 1994). Like other mouse models with diminished p53 activity, most of the tumors (13/20; 65%) were

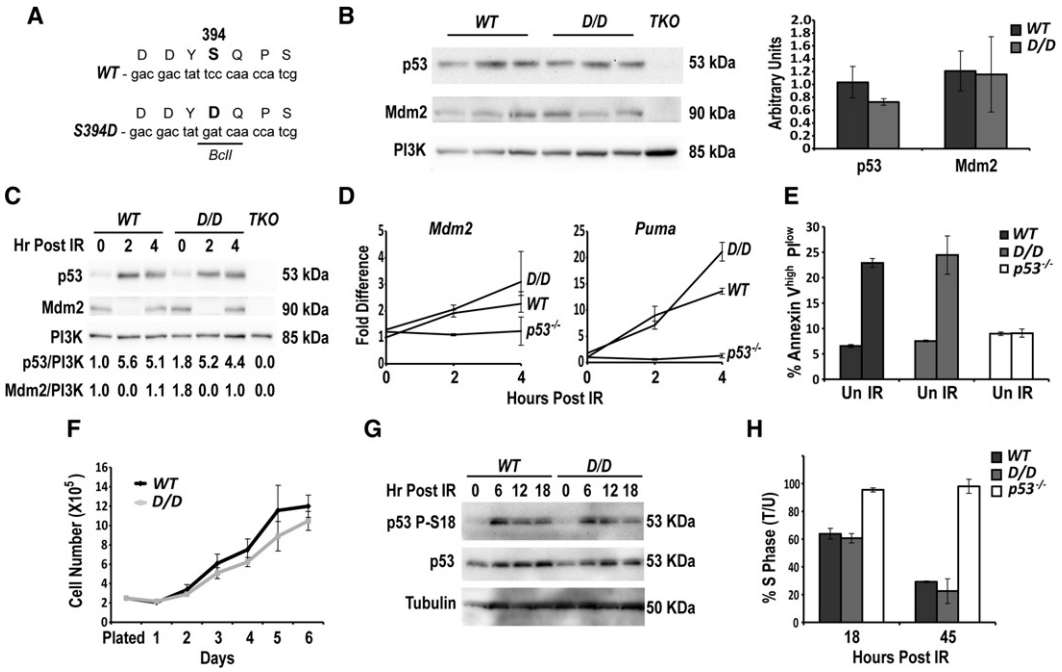

Figure 6. Phosphorylation of Mdm2 Ser394 Is Necessary But Not Sufficient to Stabilize and Activate p53

(A) DNA sequence of both the *WT* and *S394D* allele at *Mdm2* codon 394. The mutations in *S394D* also introduce a *BclI* restriction digest site.

(B) Protein levels from whole thymus extracts from untreated mice were analyzed by western blot (n = 3 per genotype). Quantified levels of p53 (p = 0.10) and Mdm2 (p = 0.88) relative to PI3K were normalized to wild-type.

(C) Mice were either untreated or irradiated with 4Gy and thymi were harvested at the indicated times. Protein levels were then analyzed by western blot. Quantified levels of p53 and Mdm2 relative to PI3K were normalized to untreated wild-type.

(D) Ex vivo thymocytes were either untreated or irradiated with 2Gy for 2 or 4 hr (n = 3 per genotype). Relative expression of *Mdm2* and *Puma* was determined by qRT-PCR. Data are presented as the ratio of mRNA to *Gapdh* mRNA. Standard deviation indicated by error bars.

(E) Ex vivo thymocytes were isolated and were either left untreated or irradiated with 2Gy for 12 hr (n = 3 per genotype). Apoptotic cells were quantified by flow cytometry. Standard deviation indicated by error bars.

(F) Primary MEF proliferation was counted each day (n = 3 per genotype). Standard deviation indicated by error bars.

(G) Primary MEFs were either untreated or irradiated with 4Gy for the indicated times, and protein levels were analyzed by western blot.

(H) Primary MEFs were treated with 4Gy IR for 18 hr or 8Gy IR for 45 hr and incubated with BrdU for 3 hr (n = 3 per genotype). Cells were then analyzed by flow cytometry. Standard deviation indicated by error bars.

See also Figure S6.

found to be T cell-derived lymphomas as determined by morphology, negative staining for the B cell marker B220, and positive staining for the T cell marker CD3 (Figure 8B, left panels). The remaining *A/A* tumors displayed severe splenomegaly and cellular infiltration in the liver and kidneys. One of these tumors stained positive for B220 and displayed expansion of the white pulp in the spleen, indicative of B cell lymphoma (Figure 8B, right panels). Sequencing of *p53* transcripts isolated from four randomly selected tumors indicated wild-type *p53* expression levels and no *p53* mutations in these *A/A* samples. These results reveal that posttranslational modification of Mdm2 Ser394 impacts p53-mediated tumor suppression as well as the p53 DNA damage response in vivo.

DISCUSSION

In our present study utilizing mouse models of Mdm2 Ser394 phosphorylation, we provide direct evidence that ATM phosphorylation of Mdm2 Ser394 regulates the ability of Mdm2 to destabilize p53 in vivo, and that this signaling impacts p53-mediated apoptosis and tumor suppression. *S394A* mice lack p53-dependent physiological responses in radiosensitive organs after IR treatment resulting in phenotypes that nearly match those seen in IR treated $p53^{-/-}$ mice: radioresistance, greatly reduced p53 target gene induction, and greatly reduced apoptosis. Importantly, the differences between *A/A* and *WT* mice were seen only in irradiated mice and tissues, as baseline levels were similar in all assays. This owes to the conservation of Mdm2 structure and function in the S394A protein, and indicates that the only difference between the wild-type and mutant Mdm2 protein is the phosphorylation status of Ser394 after cellular stress. It is likely that the compromised p53 transactivation and the reduced number of cells undergoing apoptosis and cell cycle arrest are due to the lack of p53 protein accumulation in DNA damaged *A/A* cells. Thus, phosphorylation of Mdm2 Ser394 by the ATM kinase is a major regulator of p53 stability and the subsequent p53-mediated DNA damage response in multiple tissue types.

Although loss of Mdm2 Ser394 phosphorylation greatly reduced p53-mediated apoptosis in lymphocytes and growth arrest in MEFs, it did not completely abrogate these responses (as seen in $p53^{-/-}$ mice). As anticipated by the literature, other

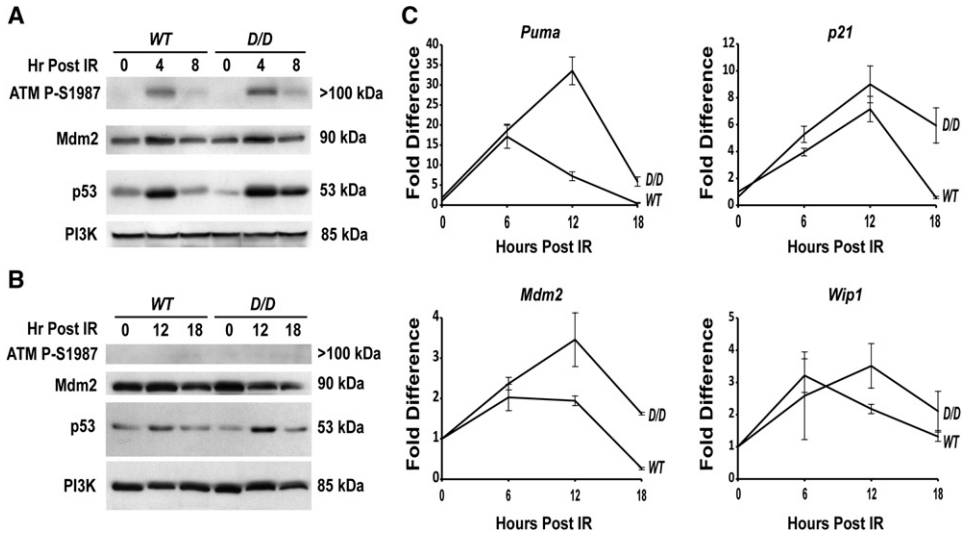

Figure 7. Mdm2 Ser394 Phosphorylation Regulates the Attenuation of the p53 Response to DNA Damage

(A) Mice were either untreated or irradiated with 4Gy and spleens were harvested either 4 or 8 hr later. Protein levels were then analyzed by western blot.

(B) Ex vivo thymocytes were either untreated or irradiated with 2Gy for either 12 or 18 hr. Protein levels were then analyzed by western blot.

(C) Ex vivo thymocytes were either untreated or irradiated with 2Gy for the indicated times (n = 3 per genotype). Relative expression levels of p53 target genes were determined by qRT-PCR. Data are presented as the ratio of mRNA to *Gapdh* mRNA. Standard deviation indicated by error bars.

See also Figure S7.

modifications to Mdm2, MdmX, and p53 must also assist in regulating p53 functions after DNA damage (Chao et al., 2003, 2006; Sluss et al., 2004; Wang et al., 2009). In agreement with this hypothesis, it is interesting to note the lack of p53 stabilization or p53 target gene activation in *D/D* mice and cells in the absence of IR treatment (Figures 6B–6D). Although the absence of a p53 response in undamaged *D/D* cells may reflect the inability of the substituted aspartate residue to perfectly mimic a phosphorylated serine residue (due to differences in the size and overall negative charge of these residues), equivalent levels of p53-mediated apoptosis and growth arrest are seen in *WT* and *D/D* cells after DNA damage. Therefore, other DNA-damage induced signals in addition to Mdm2-S394 phosphorylation are required to fully activate the DNA damage response. This interpretation also accounts for the viability of the *S394D* model, and the similar growth characteristics of nondamaged *WT*, *A/A*, and *D/D* MEFs. Collectively, our results indicate that ATM phosphorylation of Mdm2 Ser394 is necessary but not sufficient to induce a robust p53 response to IR.

Although the levels of p53 induction and activation are equivalent at early time points after IR in *WT* and *D/D* cells, p53 protein levels and activities remain elevated in *D/D* cells at later time points after IR treatment (Figures 7 and S7). In contrast, the DNA damage response in wild-type cells begins to wane after 6 hr post-IR, coincident with the induction of *Wip1* expression (Figures 7B and 7C). Because Wip1 is unable to dephosphorylate the Mdm2 S394D residue, elevation of p53 functions in *D/D* cells at later time points after IR indicates that Mdm2-S394 phosphorylation also regulates the duration of the p53 response. However, p53 levels and activities eventually return to baseline in the *D/D* cells, possibly due to the eventual loss of other secondary modifications to Mdm2 or p53. These findings are in keeping with a proposed role for Wip1 as gatekeeper of the Mdm2-p53 autoregulatory loop (Lu et al., 2007).

Interestingly, p53 tumor suppressor function is deficient in untreated *A/A* mice, as 65% of these mice developed spontaneous lymphomagenesis in the absence of exogenous IR treatment. Because our data indicate that p53 levels and activities are identical between *WT* and *A/A* cells in the absence of DNA damage, the stochastic nature of endogenous DNA damage signaling arising from inappropriate oncogene activation or DNA replication errors may account for this rather long latency period. Tumor formation in our *A/A* model is in keeping with previous reports of a role for ATM-p53 signaling and p53 activation of the proapoptotic gene *Puma* in p53-mediated suppression of lymphoma formation (Jeffers et al., 2003; Sluss et al., 2010). Likewise, the reduced capacity of p53 to suppress growth after DNA damage in *A/A* cells may also contribute to the spontaneous tumorigenic phenotype of *A/A* mice. It remains to be seen if phosphorylation of Mdm2 Ser394 by ATM also regulates p53-mediated suppression of tumors induced by sublethal doses of radiation or the forced expression of activated oncogenes.

Transfection-based experiments have determined that mutation of six separate ATM phosphorylation sites in the carboxy-terminus of MDM2, including Ser395, alters MDM2 protein oligomerization, E3-ligase activity, and the interaction of MDM2 with p53 (Cheng et al., 2009, 2011). Because p53 activity is not totally ablated in the *A/A* model, these additional ATM targets on Mdm2 may contribute to full p53 activation after DNA damage. Furthermore, a recent study found that ATM phosphorylation of MDM2 Ser395 led to increased *p53* mRNA translation, which suggests that MDM2 may be necessary for p53 protein upregulation after DNA damage (Gajjar et al., 2012). Diminished Mdm2 E3 ligase activity and phospho-Mdm2-dependent upregulation of p53 would each explain the

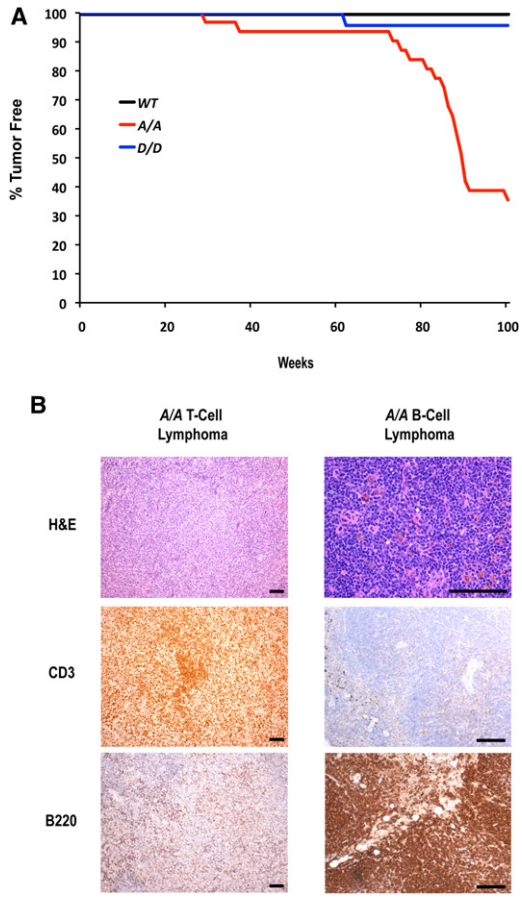

Figure 8. Phosphorylation of Mdm2 Ser394 Impacts p53 Tumor Suppression in Mice

(A) Spontaneous tumorigenesis in wild-type (n = 50), *A/A* (n = 31), and *D/D* (n = 24) mice.

(B) Representative tumor sections from an *A/A* T cell lymphoma (mesenteric lymph node, *left*) and an *A/A* B cell lymphoma (spleen, *right*). Tissue sections were stained with hematoxylin and eosin (H&E), anti-CD3, or anti-B220. Scale bars represent 100 μm.

seemingly paradoxical results of having decreased p53 levels and activities in the absence of increased Mdm2 protein in IR-treated *A/A* thymus extracts. These mechanisms would also explain the increased p53 activation at later times of the DNA damage response in *D/D* cells despite nearly equivalent levels of Mdm2 compared to wild-type. Our in vivo data are in keeping with both of these proposed models and confirm a significant role for Mdm2 S394 phosphorylation in the p53 DNA damage response.

In conclusion, our study reveals that ATM phosphorylation of Mdm2 at serine residue 394 is a critical regulator of Mdm2-p53 signaling. Phosphorylation of this Mdm2 residue by ATM following DNA damage is necessary for p53 stabilization, thereby upregulating p53 activity and activating p53 downstream functions in primary cells and tissues. Furthermore, the phosphorylation status of Mdm2 Ser394 governs the duration of the p53 response, underscoring the importance of this single phosphorylation target in regulating Mdm2-p53 signaling and p53-mediated tumor suppression. Full understanding of the multiple posttranslational modifications that influence p53 signaling will likely assist in developing better molecular diagnostics and therapeutics for human cancer patients.

EXPERIMENTAL PROCEDURES

Generation of *S394A* and *S394D* Mice

The targeting constructs contain a subcloned fragment of the *Mdm2* genomic sequence (129Sv strain). Site-directed mutagenesis was performed (Stratagene #200523). The targeting vectors were sequenced to ensure that no unwanted mutations were introduced. PC3 ES cells were electroporated with each targeting vector. Homologous recombination was detected by Southern blot using 5′ and 3′ external probes after *SpeI* and BamHI restriction digests, respectively. Targeted cells were microinjected into E3.5 blastocysts (C57BL/6 strain), and the embryos were surgically implanted into pseudopregnant foster mice by standard procedures. Transmission of the knock-in allele and excision of the neo cassette in F_1 offspring of male chimeric mice was confirmed by digestion with EcoRI followed by Southern analysis using a 3′ internal probe described previously (Steinman and Jones, 2002).

Mice

All mice used in this study were on a mixed 129Sv × C57Bl/6 background. Genomic PCR followed by either *BcgI* (*S394A*) or *BclI* (*S394D*) digestion was used to identify inheritance of the mutant alleles. Sequencing of DNA samples was performed by Sequegen. All mice and cells were irradiated with a cesium-137 source (Gammacell 40). Animals in the spontaneous tumor cohorts or IR-treated cohorts were killed if tumor burden was apparent or when moribund. Animals were maintained and used in accordance with federal guidelines and those established by the Institutional Animal Care and Use Committee at the University of Massachusetts Medical School.

Histology

Tissues were fixed in 10% formalin. Irradiated tissue sections (5 μm) were stained with anti-cleaved caspase-3 antibody (Cell Signaling #9661) or stained for TUNEL using the In Situ Cell Death Detection Kit, POD (Roche 11684817910). Tumor samples were stained with anti-CD3 (Abcam ab16044) or anti-CD45R/B220 (BD Pharmingen). All staining was performed by the UMMS Diabetes and Endocrinology Research Center Morphology Core.

Western Blotting and Reagents

Tissues and cells were lysed in NP-40 lysis buffer (50 mM Tris-HCl, pH 7.5; 150 mM NaCl; 0.5% NP-40; 20% glycerol) supplemented with 1× protease inhibitor cocktail (Roche). Protein extracts were analyzed by standard western blotting with the following antibodies: p53 (1C12), phospho-Atm Ser1987 (10H11.E12), and phospho-p53 Ser18 (#9284) from Cell Signaling; Mdm2 (mix of sc-812 and sc-1022) and lamin A/C (sc-6215) from Santa Cruz; MdmX (MDMX-82) and tubulin (T5168) from Sigma; PI3K (#06-496) from Upstate; actin (ab8229) from Abcam. Nutlin-3a (N6287) and cycloheximide (C4859) were from Sigma. PI3K and tubulin were used as loading controls. KU55933 (118502) was from Calbiochem. The CIP (M0290) and phosphatase treatment protocol were from NEB. Cellular fractionation was performed according to the manufacturer's protocol from the NE-PER Nuclear and Cytoplasmic Extraction Kit (78833) from Thermo Scientific. Protein levels in Figure 3C were quantified by densitometry using the ImageJ software. All other protein quantification was performed using the Chemidoc XRS+ Molecular Imaging System from BioRad.

Quantitative Real Time PCR

Total mRNA was isolated according to the Trizol Reagent protocol (Invitrogen) and cDNA was generated using the SuperScript II First Strand Synthesis Kit (Invitrogen). The following primers were used in qRT-PCR:

p21: 5′-TGAGGAGGAGCATGAATGGAGACA-3′
5′-AACAGGTCGGACATCACCAGGATT-3′,
Puma: 5′-CCTGGAGGGTCATGTACAATCT-3′
5′-TGCTACATGGTGCAGAAAAAGT-3′,

Bax: 5′-CTGAGCTGACCTTGGAGC-3′
5′-GACTCCAGCCACAAAGATG-3′,
Noxa: 5′-CCACCTGAGTTCGCAGCTCAA-3′
5′-GTTGAGCACACTCGTCCTTCA-3′,
Mdm2: 5′-GCATTCTGGTGATTGCCTGGATCA-3′
5′-AGACTGTGACCCGATAGACCTCAT-3′
Gapdh: 5′-TGGCAAAGTGGAGATTGTTGCC-3′
5′-AAGATGGTGATGGGCTTCCCG-3′.

All data are presented as the ratio of mRNA to *Gapdh* mRNA.

For the QIAGEN p53 PCR Array experiments, mRNA was isolated using the RNeasy kit (74104) with DNase (79254) from QIAGEN. cDNA was synthesized using the RT2 First Strand Kit (330401) from QIAGEN. p53 PCR Arrays (PAMM-027C) were run according to manufacturer's protocol using the RT2 SYBR Green ROX qPCR Mastermix (330520) from QIAGEN.

Flow Cytometry

For apoptosis, samples were treated according to the Annexin V-FITC Apoptosis Detection Kit I protocol (BD Pharmingen #556547). Early apoptotic cells (Annexin V^{high} PI^{low}) were quantitated and presented. For cell cycle arrest, treated MEFs were pulsed labeled with 60 μM bromodeoxyuridine (BrdU) for 3 hr. Cells were then trypsinized, fixed in 70% ethanol overnight, incubated with anti-BrdU antibody (Becton Dickinson #347583) and PI, and analyzed by flow cytometry. Data are presented as the percentage of cells in S phase in the treated samples compared to the untreated samples. Flow cytometry was performed by the UMASS Medical School Flow Cytometry Core Lab.

SUPPLEMENTAL INFORMATION

Supplemental Information includes seven figures and can be found with this article online at doi:10.1016/j.ccr.2012.04.011.

ACKNOWLEDGMENTS

We thank Marilyn Keeler and Judith Gallant for help with the ES cell and blastocyst injection experiments, and Lawrence Donehower for comments on the manuscript. Core facilities were partly supported by grant DK32520 from the NIDDK. This research was supported by grant CA077735 from the National Cancer Institute (S.N.J.).

Received: August 18, 2011
Revised: December 13, 2011
Accepted: April 3, 2012
Published: May 14, 2012

REFERENCES

Bond, G.L., Hu, W., and Levine, A.J. (2005). MDM2 is a central node in the p53 pathway: 12 years and counting. Curr. Cancer Drug Targets *5*, 3–8.

Chao, C., Saito, S., Anderson, C.W., Appella, E., and Xu, Y. (2000). Phosphorylation of murine p53 at ser-18 regulates the p53 responses to DNA damage. Proc. Natl. Acad. Sci. USA *97*, 11936–11941.

Chao, C., Hergenhahn, M., Kaeser, M.D., Wu, Z., Saito, S., Iggo, R., Hollstein, M., Appella, E., and Xu, Y. (2003). Cell type- and promoter-specific roles of Ser18 phosphorylation in regulating p53 responses. J. Biol. Chem. *278*, 41028–41033.

Chao, C., Herr, D., Chun, J., and Xu, Y. (2006). Ser18 and 23 phosphorylation is required for p53-dependent apoptosis and tumor suppression. EMBO J. *25*, 2615–2622.

Chen, J., Lin, J., and Levine, A.J. (1995). Regulation of transcription functions of the p53 tumor suppressor by the mdm-2 oncogene. Mol. Med. *1*, 142–152.

Cheng, Q., Chen, L., Li, Z., Lane, W.S., and Chen, J. (2009). ATM activates p53 by regulating MDM2 oligomerization and E3 processivity. EMBO J. *28*, 3857–3867.

Cheng, Q., Cross, B., Li, B., Chen, L., Li, Z., and Chen, J. (2011). Regulation of MDM2 E3 ligase activity by phosphorylation after DNA damage. Mol. Cell. Biol. *31*, 4951–4963.

Donehower, L.A., Harvey, M., Slagle, B.L., McArthur, M.J., Montgomery, C.A., Jr., Butel, J.S., and Bradley, A. (1992). Mice deficient for p53 are developmentally normal but susceptible to spontaneous tumours. Nature *356*, 215–221.

Gajjar, M., Candeias, M.M., Malbert-Colas, L., Mazars, A., Fujita, J., Olivares-Illana, V., and Fåhraeus, R. (2012). The p53 mRNA-Mdm2 interaction controls Mdm2 nuclear trafficking and is required for p53 activation following DNA damage. Cancer Cell *21*, 25–35.

Gudkov, A.V., and Komarova, E.A. (2003). The role of p53 in determining sensitivity to radiotherapy. Nat. Rev. Cancer *3*, 117–129.

Gurley, K.E., and Kemp, C.J. (2007). Ataxia-telangiectasia mutated is not required for p53 induction and apoptosis in irradiated epithelial tissues. Mol. Cancer Res. *5*, 1312–1318.

Harvey, M., McArthur, M.J., Montgomery, C.A., Jr., Butel, J.S., Bradley, A., and Donehower, L.A. (1993). Spontaneous and carcinogen-induced tumorigenesis in p53-deficient mice. Nat. Genet. *5*, 225–229.

Hickson, I., Zhao, Y., Richardson, C.J., Green, S.J., Martin, N.M., Orr, A.I., Reaper, P.M., Jackson, S.P., Curtin, N.J., and Smith, G.C. (2004). Identification and characterization of a novel and specific inhibitor of the ataxia-telangiectasia mutated kinase ATM. Cancer Res. *64*, 9152–9159.

Hollstein, M., Sidransky, D., Vogelstein, B., and Harris, C.C. (1991). p53 mutations in human cancers. Science *253*, 49–53.

Honda, R., Tanaka, H., and Yasuda, H. (1997). Oncoprotein MDM2 is a ubiquitin ligase E3 for tumor suppressor p53. FEBS Lett. *420*, 25–27.

Jack, M.T., Woo, R.A., Hirao, A., Cheung, A., Mak, T.W., and Lee, P.W. (2002). Chk2 is dispensable for p53-mediated G1 arrest but is required for a latent p53-mediated apoptotic response. Proc. Natl. Acad. Sci. USA *99*, 9825–9829.

Jacks, T., Remington, L., Williams, B.O., Schmitt, E.M., Halachmi, S., Bronson, R.T., and Weinberg, R.A. (1994). Tumor spectrum analysis in p53-mutant mice. Curr. Biol. *4*, 1–7.

Jeffers, J.R., Parganas, E., Lee, Y., Yang, C., Wang, J., Brennan, J., MacLean, K.H., Han, J., Chittenden, T., Ihle, J.N., et al. (2003). Puma is an essential mediator of p53-dependent and -independent apoptotic pathways. Cancer Cell *4*, 321–328.

Jones, S.N., Hancock, A.R., Vogel, H., Donehower, L.A., and Bradley, A. (1998). Overexpression of Mdm2 in mice reveals a p53-independent role for Mdm2 in tumorigenesis. Proc. Natl. Acad. Sci. USA *95*, 15608–15612.

Jones, S.N., Roe, A.E., Donehower, L.A., and Bradley, A. (1995). Rescue of embryonic lethality in Mdm2-deficient mice by absence of p53. Nature *378*, 206–208.

Juven, T., Barak, Y., Zauberman, A., George, D.L., and Oren, M. (1993). Wild type p53 can mediate sequence-specific transactivation of an internal promoter within the mdm2 gene. Oncogene *8*, 3411–3416.

Kemp, C.J., Wheldon, T., and Balmain, A. (1994). p53-deficient mice are extremely susceptible to radiation-induced tumorigenesis. Nat. Genet. *8*, 66–69.

Khosravi, R., Maya, R., Gottlieb, T., Oren, M., Shiloh, Y., and Shkedy, D. (1999). Rapid ATM-dependent phosphorylation of MDM2 precedes p53 accumulation in response to DNA damage. Proc. Natl. Acad. Sci. USA *96*, 14973–14977.

Komarova, E.A., Kondratov, R.V., Wang, K., Christov, K., Golovkina, T.V., Goldblum, J.R., and Gudkov, A.V. (2004). Dual effect of p53 on radiation sensitivity in vivo: p53 promotes hematopoietic injury, but protects from gastro-intestinal syndrome in mice. Oncogene *23*, 3265–3271.

Lane, D.P. (1992). Cancer. p53, guardian of the genome. Nature *358*, 15–16.

Levine, A.J., Tomasini, R., McKeon, F.D., Mak, T.W., and Melino, G. (2011). The p53 family: guardians of maternal reproduction. Nat. Rev. Mol. Cell Biol. *12*, 259–265.

Lu, X., Nannenga, B., and Donehower, L.A. (2005). PPM1D dephosphorylates Chk1 and p53 and abrogates cell cycle checkpoints. Genes Dev. *19*, 1162–1174.

Lu, X., Ma, O., Nguyen, T.A., Jones, S.N., Oren, M., and Donehower, L.A. (2007). The Wip1 Phosphatase acts as a gatekeeper in the p53-Mdm2 autoregulatory loop. Cancer Cell *12*, 342–354.

Lu, X., Nguyen, T.A., Moon, S.H., Darlington, Y., Sommer, M., and Donehower, L.A. (2008). The type 2C phosphatase Wip1: an oncogenic regulator of tumor suppressor and DNA damage response pathways. Cancer Metastasis Rev. *27*, 123–135.

Maya, R., Balass, M., Kim, S.T., Shkedy, D., Leal, J.F., Shifman, O., Moas, M., Buschmann, T., Ronai, Z., Shiloh, Y., et al. (2001). ATM-dependent phosphorylation of Mdm2 on serine 395: role in p53 activation by DNA damage. Genes Dev. *15*, 1067–1077.

Momand, J., Zambetti, G.P., Olson, D.C., George, D., and Levine, A.J. (1992). The mdm-2 oncogene product forms a complex with the p53 protein and inhibits p53-mediated transactivation. Cell *69*, 1237–1245.

Montes de Oca Luna, R., Wagner, D.S., and Lozano, G. (1995). Rescue of early embryonic lethality in mdm2-deficient mice by deletion of p53. Nature *378*, 203–206.

O'Gorman, S., Dagenais, N.A., Qian, M., and Marchuk, Y. (1997). Protamine-Cre recombinase transgenes efficiently recombine target sequences in the male germ line of mice, but not in embryonic stem cells. Proc. Natl. Acad. Sci. USA *94*, 14602–14607.

Pellegrini, M., Celeste, A., Difilippantonio, S., Guo, R., Wang, W., Feigenbaum, L., and Nussenzweig, A. (2006). Autophosphorylation at serine 1987 is dispensable for murine Atm activation in vivo. Nature *443*, 222–225.

Shieh, S.Y., Ikeda, M., Taya, Y., and Prives, C. (1997). DNA damage-induced phosphorylation of p53 alleviates inhibition by MDM2. Cell *91*, 325–334.

Shreeram, S., Demidov, O.N., Hee, W.K., Yamaguchi, H., Onishi, N., Kek, C., Timofeev, O.N., Dudgeon, C., Fornace, A.J., Anderson, C.W., et al. (2006). Wip1 phosphatase modulates ATM-dependent signaling pathways. Mol. Cell *23*, 757–764.

Sluss, H.K., Armata, H., Gallant, J., and Jones, S.N. (2004). Phosphorylation of serine 18 regulates distinct p53 functions in mice. Mol. Cell. Biol. *24*, 976–984.

Sluss, H.K., Gannon, H., Coles, A.H., Shen, Q., Eischen, C.M., and Jones, S.N. (2010). Phosphorylation of p53 serine 18 upregulates apoptosis to suppress Myc-induced tumorigenesis. Mol. Cancer Res. *8*, 216–222.

Soussi, T., and Béroud, C. (2001). Assessing TP53 status in human tumours to evaluate clinical outcome. Nat. Rev. Cancer *1*, 233–240.

Steinman, H.A., and Jones, S.N. (2002). Generation of an Mdm2 conditional allele in mice. Genesis *32*, 142–144.

Stommel, J.M., and Wahl, G.M. (2004). Accelerated MDM2 auto-degradation induced by DNA-damage kinases is required for p53 activation. EMBO J. *23*, 1547–1556.

Vassilev, L.T., Vu, B.T., Graves, B., Carvajal, D., Podlaski, F., Filipovic, Z., Kong, N., Kammlott, U., Lukacs, C., Klein, C., et al. (2004). In vivo activation of the p53 pathway by small-molecule antagonists of MDM2. Science *303*, 844–848.

Vousden, K.H., and Lu, X. (2002). Live or let die: the cell's response to p53. Nat. Rev. Cancer *2*, 594–604.

Wang, Y.V., Leblanc, M., Wade, M., Jochemsen, A.G., and Wahl, G.M. (2009). Increased radioresistance and accelerated B cell lymphomas in mice with Mdmx mutations that prevent modifications by DNA-damage-activated kinases. Cancer Cell *16*, 33–43.

Wu, X., Bayle, J.H., Olson, D., and Levine, A.J. (1993). The p53-mdm-2 autoregulatory feedback loop. Genes Dev. *7* (7A), 1126–1132.

Wu, Z., Earle, J., Saito, S., Anderson, C.W., Appella, E., and Xu, Y. (2002). Mutation of mouse p53 Ser23 and the response to DNA damage. Mol. Cell. Biol. *22*, 2441–2449.